Chemistry Europe
European Chemical Societies Publishing

WILEY VCH

Excellence in Chemistry Research

Announcing our new flagship journal

- Gold Open Access
- Publishing charges waived
- Preprints welcome
- Edited by active scientists

Meet the Editors of *ChemistryEurope*

Luisa De Cola
Università degli Studi di Milano Statale, Italy

Ive Hermans
University of Wisconsin-Madison, USA

Ken Tanaka
Tokyo Institute of Technology, Japan

Chemistry–A European Journal
Research Article
doi.org/10.1002/chem.202202672
Chemistry Europe
European Chemical Societies Publishing
www.chemeurj.org

Sterically and Electronically Flexible Pyridylidene Amine Dinitrogen Ligands at Palladium: Hemilabile *cis*/*trans* Coordination and Application in Dehydrogenation Catalysis

Nicolas Lentz,[a] Yanik Streit,[a] Pascal Knörr,[a] and Martin Albrecht*[a]

Dedicated to Gerard van Koten on the occasion of his 80th birthday and in admiration of his pioneering work on pincer chemistry.

Abstract: Ligand design is crucial for the development of new catalysts and materials with new properties. Herein, the synthesis and unique hemilabile coordination properties of new bis-pyridylidene amine (bis-PYE) ligands to palladium, and preliminary catalytic activity of these complexes in formic acid dehydrogenation are described. The synthetic pathway to form cationic complexes [Pd(bis-PYE)Cl(L)]X with a *cis*-coordinated *N,N*-bidentate bis-PYE ligand is flexible and provides access to a diversity of Pd^{II} complexes with different ancillary ligands (L = pyridine, DMAP, PPh_3, Cl, $P(OMe)_3$). The ^1H NMR chemical shift of the *trans*-positioned PYE N–CH_3 unit is identified as a convenient and diagnostic handle to probe the donor properties of these ancillary ligands and demonstrates the electronic flexibility of the PYE ligand sites. In the presence of a base, the originally *cis*-coordinated bis-PYE ligand adopts a *N,N,N*-tridentate coordination mode with the two PYE units in mutual *trans* position. This *cis*–*trans* isomerization is reverted in presence of an acid, demonstrating a unique structural and steric flexibility of the bis-PYE ligand at palladium in addition to its electronic adaptability. The palladium complexes are active in formic acid dehydrogenation to H_2 and CO_2. The catalytic performance is directly dependent on the ligand bonding mode, the nature of the ancillary ligand, the counteranion, and additives. The most active system features a bidentate bis-PYE ligand, PPh_3 as ancillary ligand and accomplishes turnover frequencies up to 525 h^{-1} in the first hour and turnover numbers of nearly 1000, which is the highest activity reported for palladium-based catalysts to date.

Introduction

Nitrogen-based ligands are ubiquitous in coordination chemistry due to their immense versatility, including neutral nitriles, imines, and amines, as well as anionic amido (R_2N^-), imido (RN^{2-}), and nitrido (N^{3-}) ligands.[1] A rather recent addition to these classes of nitrogen ligands are the so-called pyridylidene-amines (PYEs),[2,3] which can be represented by either a limiting zwitterionic resonance structure A or a neutral quinoidal structure B (Figure 1a). Hence, this ligand is ambivalent and constitutes a link between the classes of neutral and ionic nitrogen ligands. Moreover, it has been demonstrated that the contribution of the two limiting structures can be altered by several factors including the electron density of the metal center (modification of oxidation state, ancillary ligands) as well as reaction media. This modularity imparts unique electronic flexibility to this ligand as it allows to toggle between a π-basic and a π-acidic donor site.[4,5] The flexibility is evidenced, for example, by NMR spectroscopy thought the variable shift difference of the H_α and H_β resonances,[6] and also by X-ray

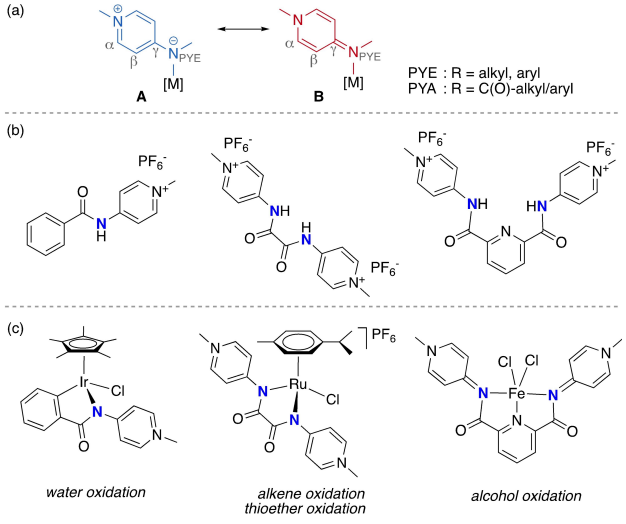

Figure 1. (a) Limiting resonance structures of PYA/PYE ligands featuring an anionic or a neutral coordination site; (b) examples of mono-, bi-, and tridentate PYA/PYE ligand precursors; (c) representative PYA complexes with catalytic activity.

[a] Dr. N. Lentz, Y. Streit, P. Knörr, Prof. Dr. M. Albrecht
Department of Chemistry, Biochemistry and Pharmaceutical Sciences
University of Bern, Freiestrasse 3, CH-3012 Bern (Switzerland)
E-mail: martin.albrecht@unibe.ch

Supporting information for this article is available on the WWW under https://doi.org/10.1002/chem.202202672

diffraction, which reveals variable degrees of double bond localization by analysis of the C_α–C_β, C_β–C_γ, and the exocyclic C_γ–N_{PYE} bond lengths.[7]

Over the last decade and following the pioneering work of Johnson and Douthwaite,[2,8] a variety of PYE ligands have been developed from inexpensive starting materials, featuring mono-, bi-, and tridentate metal bonding (Figure 1b).[3] In addition, pyridylidene amides (PYAs) were introduced by Wright and coworkers as a variation that features a carbonyl as opposed to an alkyl or aryl substituent at the exocyclic nitrogen.[8,9] More recently, our group extended the PYA library with the implementation of highly versatile and modular pincer-type pyridine bis-PYA ligands that coordinate to both noble and base metals in various oxidation states. Some of these complexes have been used for catalytic redox reactions, for example, transfer hydrogenation,[10] C–F bond activation,[8] and the oxidation of water,[7] alcohols,[11] alkenes,[12] sulfides,[13] in some cases with extraordinary performance.[12]

Here, we describe a new addition to the PYE family, namely a bis-PYE system with the two PYE units linked through a phenyl-NH-phenyl linker. The presence of the NH unit imparts hemilability,[14] and reversible switching between bidentate and tridentate coordination as exemplified in palladium(II) complexes. This modular coordination mode arranges the two PYE ligand sites in either mutual *cis* or *trans* position and adds a further dimension of flexibility on top of the electronic flexibility of the PYE sites (Figure 1a). The relevance of the ligand setup is further demonstrated here in the catalytic dehydrogenation of formic acid. The new bis-PYE palladium complexes reach catalytic activity that is unusually high for group 10 metal systems.[15–17]

Results and Discussion

Synthesis of the complexes

The bis-PYE ligand precursor **1** was obtained by preparing first the N,N,N scaffold via a known[18] two-step procedure from commercially available 2-nitroaniline and 2-fluoroaniline and subsequent condensation with 4-chloropyridinium triflate under neat reaction conditions at 160 °C (Scheme 1). Subsequent anion metathesis with an excess of aqueous NH_4PF_6 afforded bis-PYE ligand precursor **1**, which features a characteristic N–CH_3 chemical shift at $\delta_H = 4.12$. Deprotonation of **1** with aqueous KOH afforded the neutral bis-PYE **2** in quantitative yields. The N–CH_3 resonance shifted upfield upon deprotonation and appears at $\delta_H = 3.49$ due to a higher contribution of the neutral quinoidal resonance form.

Coordination of the new bis-PYE ligand to palladium was accomplished by reacting the bis-pyridinium salt **1** with $Pd(PPh_3)_2Cl_2$ in the presence of diazabicycloundecene (DBU) as a base, which induced displacement of a PPh_3 and chloride ligand by the bis-PYE and formation of complex **3a** as an orange powder in 81% yield. Complex **3a** is air- and moisture-stable for weeks.

Analogous palladation of the neutral bis-PYE ligand **2** in the absence of an auxiliary base yielded complex **3b** with a non-coordinating chloride counterion in 92% yield. Halide abstraction of **3b** with $AgPF_6$ led to the quantitative formation of **3a**. Notably, no further reaction was observed even when an excess of $AgPF_6$ was used, indicating that the chloride in the palladium coordination sphere is tightly bound. Similar, counterion metathesis with $NaBPh_4$ gave complex **3c**, which was suitable for single crystal growth. The ^1H NMR spectra of the cationic unit of **3a**, **3b** and **3c** are identical and feature two non-equivalent PYE units, evidenced for example by non-equivalent N–CH_3 singlets at $\delta_H = 3.46$ and 3.37 ppm. This inequivalence is

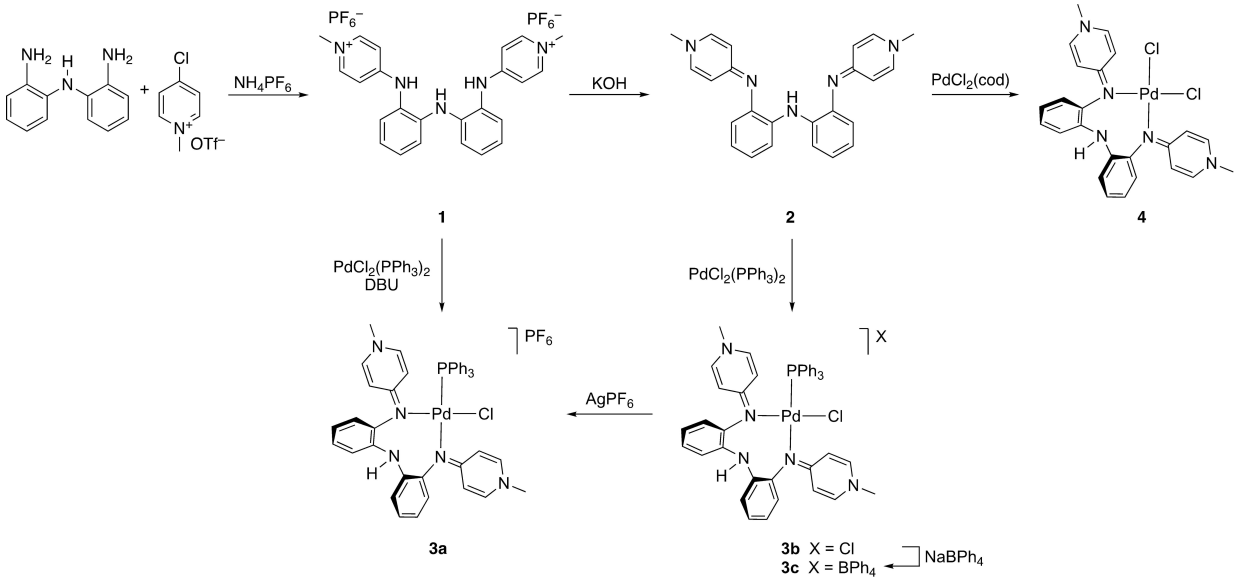

Scheme 1. Synthesis of ligand precursors **1** and **2**, and complexes **3**–**4**.

indicating two different ligands in *trans* position and therefore supports a *cis-N,N*-bidentate coordination mode of the bis-PYE ligand. The high-field shift of the N–CH_3 resonances suggests a significant contribution of the neutral quinoidal PYE resonance form and hence a localization of the positive charge predominantly on the palladium center rather than the pyridinium nitrogen. This model is corroborated by the shielded β hydrogens of the PYE heterocycle (δ_H = 5.6–6.8 ppm; see Scheme 1a for proton labeling).[8]

Palladation of the deprotonated ligand **2** with the phosphine-free metal precursor [$PdCl_2$(cod)] (cod = 1,5-cyclooctadiene) or with $PdCl_2$ yielded the neutral bis-PYE palladium complex **4** as a yellow air-stable powder (Scheme 1). The ^{1}H NMR spectrum of **4** revealed a higher symmetry of this complex with only one set of PYE signals, featuring a single N–CH_3 resonance at 3.41 ppm and high-field shifted doublets for the PYE β-hydrogens at 6.10 and 6.24 ppm. The inequivalence of these hydrogens suggests a rigid orientation of the heterocycle and a significant barrier for rotation about the N_{PYE}–C_γ bond.

Single crystals suitable for X-ray diffraction analysis were obtained from slow diffusion of pentane into a CH_2Cl_2 solution of **3c**, and by slow evaporation of a MeCN solution of **4**.[19] The molecular structures feature a palladium center in a slightly distorted square planar geometry with an acute N1–Pd1–N2 bite angle of 82.9(1)° for both complexes (Figure 2). The four aromatic rings of the bis-PYE ligand are located alternatingly above and below the palladium square plane, which results in a helix-type ligand motif (Figure S1). Obviously, the helical chirality is racemic in the absence of a chiral auxiliary, and both structures crystalized in a centrosymmetric space group where both enantiomers are symmetry-related. The Pd1–N1 and Pd–N2 bond lengths are slightly longer in **3c** (2.044(3) and 2.066(3) Å) than in **4** (2.023(5) Å), which was attributed to the *trans* influence and steric hindrance of the phosphine ligand. The C–C and C–N bond distance in the PYE heterocycles indicate considerable double bond localization with C_α–C_β bonds around 1.35(1) Å and C_β–C_γ bonds around 1.43(1) Å. Moreover, the exocyclic N_{PYE}–C_γ distances are only 1.32(1) Å, which is much shorter than the N_{PYE}–C_{Aryl} single bonds (1.42(1) Å) and commensurate with a double bond as shown in the neutral quinoidal representation of **3c** and **4** (Scheme 1).

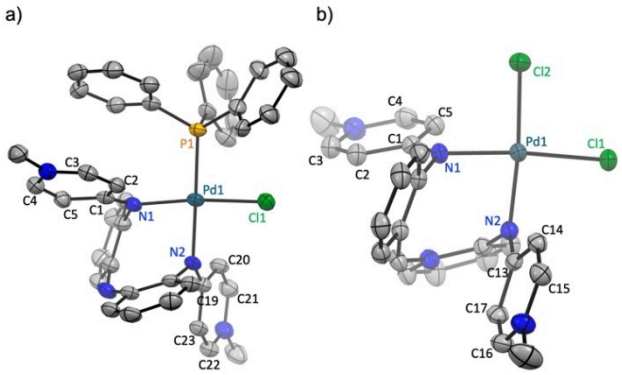

Figure 2. ORTEP representation of **3c** (a) and **4** (b) at 50% probability level (all hydrogen atoms and BPh_4 anion of **3c** omitted, rings below the coordination plane in lighter shade). Selected bond distances (Å) and bond angles (deg) for complex **3c**: Pd1–Cl1 2.3054(10), Pd1–P1 2.2757(9), Pd1–N1 2.044(3), Pd1–N2 2.068(3), N1–C18 1.432(5), N2–C7 1.412(5), N1–C1 1.313(5), N2–C19 1.322(5), C1–C2 1.425(6), C1–C5 1.423(6), C2–C3 1.351(6), C4–C5 1.351(6), C19–C23 1.430(5), C19–C20 1.432(6), C23–C22 1.356(6), C20–C21 1.347(6), P1–Pd1–Cl1 89.87(4), N1–Pd1–N2 82.90(12), N1–Pd1–P1 96.12(9), N2–Pd1–Cl1 90.04(9), C1–N1–C18 121.1(3), C7–N2–C19 121.8(3). For complex **4**: Pd1–Cl1 2.3285(5), Pd1–Cl2 2.3168(6), Pd1–N1 2.0202(18), Pd1–N2 2.0256(18), N1–C7 1.427(5), N2–C19 1.422(3), N1–C1 1.320(3), N2–C13 1.322(3), C1–C2 1.430(3), C1–C5 1.435(3), C2–C3 1.350(3), C4–C5 1.353(3), C13–C17 1.433(3), C13–C14 1.422(3), C14–C15 1.346(3), C17–C16 1.349(3), Cl1–Pd1–Cl2 93.73(2), N1–Pd1–N2 82.89(7), N1–Pd1–Cl2 91.67(5), N2–Pd1–Cl1 91.74(5), C1–N1–C7 121.69(18), C13–N2–C19 121.81(18).

Probing the *trans* influence of ligands L

The lability of one chloride in complex **4** was exploited to introduce a series of different ancillary ligands in the complex [Pd(bis-PYE)Cl(L)] (Scheme 2). Thus, addition of pyridine to complex **4** resulted in the clean formation of complex **5** according to in situ ^{1}H NMR spectroscopy, which showed resonances for coordinated pyridine and the desymmetrization of the PYE units. The latter is most diagnostic by the appearance of two singlets due to the non-equivalent N–CH_3 groups at δ_H = 3.48 and 3.51 ppm. Attempts to isolate complex **5** afforded a mixture of **5** and **4**, however, and drying the mixture in vacuo reverted pure complex **4**, indicating labile bonding of the pyridine ligand. More basic pyridine derivatives such as *N,N*-dimethylaminopyridine (DMAP) shifted this equilibrium to the product side and gave complex **6**, which was sufficiently stable for purification. Similarly, reacting complex **4** with PPh_3 or $P(OPh)_3$ yielded complexes **3b** and **7**, respectively, indicating a high synthetic versatility. Complexes **5**–**7** were also prepared without isolating **4**, i.e., upon metalation of the deprotonated bis-PYE ligand **2** with $PdCl_2$ in the presence the corresponding ancillary ligand L. All complexes featured diagnostic non-equivalent N–CH_3 resonances (δ_H = 3.46 and 3.51 for **6**, 3.43 and 3.46 for **7**). Ligand displacement experiments indicated an increasing stability of the ancillary ligand in the sequence pyridine ≃ Cl^- < DMAP < $P(OPh)_3$ < PPh_3.

The availability of a set of palladium complexes with different ancillary ligands provided an opportunity to demonstrate the PYE's unique ability to adapt its electronic structure. This adaptability is directly dependent on the donor properties of the ancillary ligands and was probed here by the chemical

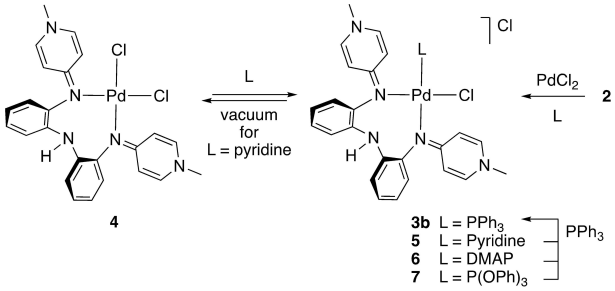

Scheme 2. Synthesis of complexes **3b**, **5**, **6** and **7**.

shift of the N–CH_3 resonance of the PYE unit *trans* to the ancillary ligand L, which was identified by 2D NOESY experiments. Previous work with PYAs used the pyridylidiene H_α and H_β resonances as probes. Even though these resonances are shifted over a larger NMR frequency range and would therefore provide a finer scale, their identification is not unambiguous in the spectra of complexes **3**–**7**. In contrast, the N–CH_3 resonances are in an uncluttered spectral range and therefore provide a more practical ^{1}H NMR spectroscopic handle (Figure 3). When considering the limiting resonance structures for a zwitterionic form, represented by the protonated ligand precursor **1** ($\delta_H = 3.93$), and the neutral quinoidal form in deprotonated bis-PYE **2** ($\delta_H = 3.36$), a trend emerges from the least to the strongest electron donor ligands along the series DMAP **6** ($\delta_H = 3.46$) < chloride **4** ($\delta_H = 3.45$) < phosphite **7** ($\delta_H = 3.43$) < phosphine **3b** ($\delta_H = 3.37$). Hence, the N–CH_3 resonance serves as a useful proxy for ranking the *trans* influence of the ancillary ligand. Notably, the *cis* N–CH_3 group remains unchanged in the dissymmetric complexes at $\delta_H = 3.46$.

Lability of the NH proton and *cis-trans* isomerization of the bis-PYE ligand

Deprotonation of the central *NH* unit in complex **3b** with KO*t*Bu gave complex **8** in excellent 96% isolated yield. Weaker bases such as NEt_3 or K_2CO_3 did not induce formation of **8**, indicating a low acidity of the *NH* proton. Complex **8** features a *N,N,N*-tridentate pincer-type[20] bis-PYE ligand with the PYE donor sites now arranged in mutual *trans* position as opposed to *cis* coordination in **3b**. This *cis-trans* isomerization is reminiscent to the coordination flexibility of the widely known Xantphos system.[21,22]

The formation of **8** was monitored by ^{31}P NMR spectroscopy through the detection of dissociated PPh_3 ($\delta_P = -5$ vs. 24.7 ppm in **3b**), indicative of a tridentate bonding mode of the bis-PYE ligand. In addition, the N*H* signal of **3b** at $\delta_H = 8.98$ ppm disappeared upon deprotonation. In agreement with a higher molecular symmetry, the ^{1}H NMR spectrum of **8** exhibits symmetry-related PYE units, for example, only a single resonance for the two N–CH_3 groups at 3.73 ppm. The downfield shift of this resonance compared to the one in complex **4** ($\delta_H = 3.45$) and in **2** ($\delta_H = 3.53$) suggests a higher contribution of the zwitterionic PYE resonance form and therefore a stronger donation of the PYE unit to the palladium center. This model is corroborated by the deshielded PYE H_β doublets at $\delta_H = 7.72$ (cf. 6.10 and 6.24 in **2**). While the formation of **8** was further supported by HRMS (m/z = 486.0878; calcd 486.0910 for $[M–Cl]^+$), we have not succeeded so far in growing X-ray diffraction quality single crystals. However, complex **8** was also synthesized from complexes **3a**–**b** and from **4** upon reaction with KO*t*Bu.

Addition of HCl to complex **8** reversed the reaction and reverted the bis-PYE ligand back to a bidentate coordination mode, cleanly affording complex **4** as indicated by the characteristic NMR spectroscopic shifts (Scheme 3). The protonation-deprotonation sequence was also performed in a sequential one-pot reaction and did not lead to any loss of complex. The full reversibility of the reaction demonstrates the hemilability of the aniline-type nitrogen coordination site and indicates a proton-triggered mechanism for the *cis-trans* isomerization of the bis-PYE sites. This feature is particularly attractive when applying this complex in bond activation reactions that entail a proton transfer step.

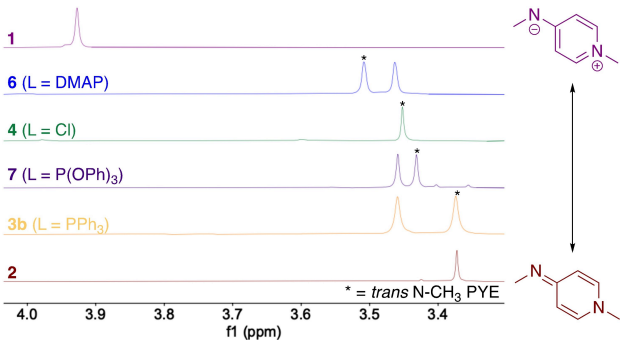

Figure 3. ^{1}H NMR spectra (CD_2Cl_2, 300 MHz) of **1** and **2**, and complexes **3b**, **4**, **6** and **7** (*trans* refers to N–CH_3 group of the PYE site *trans* to ancillary ligand L).

Formic acid dehydrogenation catalysis

The potential of these proton-responsive ligands was evaluated in the catalytic dehydrogenation of formic acid (FA). FA has attracted much interest recently as liquid organic hydrogen carrier, conveying an appealing solution for storing and transporting chemical energy to implement a hydrogen economy.[23] FA dehydrogenation catalysts have been continuously improved over the last decade, with major contributions from various groups such as those of Beller, Hazari, and Milstein.[24–28] State-of-the-art catalysts are relying predominantly on group 8 and 9 metals with phosphine-based pincer ligands.[29–31] While the use of Earth-abundant metals has become more popular over the past years,[32–35] group 10 metal complexes are scarce in FA dehydrogenation catalysis and generally feature only low performance.[15–17] The activity of the bis-PYE palladium complexes **3**–**8** was investigated in the presence of NEt_3 in dioxane at 80 °C (Table 1, S1 and Figure 4).[25,35] The non-coordinating counterion had a remarkably strong influence on the catalytic activity. While complex **3a** with a PF_6^- anion showed appreci-

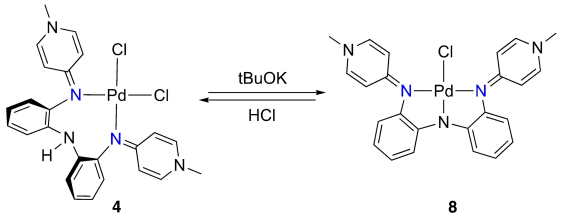

Scheme 3. Xantphos-type reversible swapping of the two PYE coordination sites from *cis* to *trans*, triggered by deprotonation of **4** and protonation of **8**.

Table 1. Catalytic dehydrogenation of FA with different palladium complexes.[a]

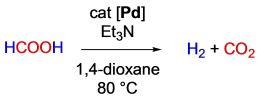

Entry	[Pd]	$V_{100\ min}$ [mL]	TON	TOF_{max} [h^{-1}][b]
1	3a	10.5	23	100
2	3b	48	100	115
3	3c	<1	<1	n.a.
4	4	28	61	400
5	6	16	35	72
6	7	20	44	72
7	8	10	22	400
8	–	<1	n.a.	n.a.
9	$Pd(PPh_3)_2Cl_2$	6	13	9
10[c]	3b	39	850	525
11[d]	3b	39	550	220

[a] Condition: catalyst (1 mol%), FA (1 mmol), Et_3N (0.91 mmol) and 1,4-dioxane (1 mL) at 80 °C for 100 min; GC analysis of the headspace confirmed the formation of H_2 and CO_2 exclusively without any detectable quantities of CO; n.a. = not applicable. [b] maximum TOF determined from the catalytic profile. [c] 0.1 mol% **3b**, 4 h reaction time. [d] 0.01 mol% **3b**, 6 h reaction time.

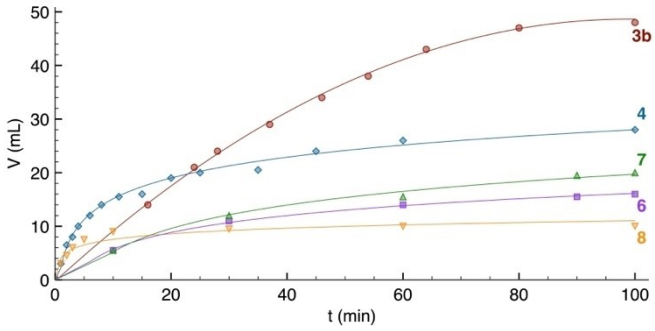

Figure 4. Time-dependent gas evolution profile from palladium-catalyzed formic acid dehydrogenation using complex **3b** (circles), **4** (diamonds), **6** (squares), **7** (triangles) and **8** (inverted triangles). Condition: catalyst (1 mol%), FA (1 mmol), Et_3N (0.91 mmol), and 1,4-dioxane (1 mL) at 80 °C.

able initial activity with maximum turnover frequency TOF_{max} = 100 h^{-1}, catalytic activity stalled at 23 turnovers (entry 1). The chloride analogue **3b** showed much higher catalytic robustness with complete conversion (turnover number, TON = 100) within 100 min and similar TOF values (entry 2). In contrast, complex **3c** with a BPh_4^- counterion was completely inactive (entry 3). The neutral complex **4** showed a considerably increased initial activity with a TOF_{max} = 400 h^{-1} (entry 4). However, catalytic activity decreased substantially after some 10 min, pointing to some catalyst deactivation, and giving only 60 TONs. Substitution of the ancillary phosphine ligand in **3b** by DMAP or $P(OPh)_3$) was deleterious to catalytic activity and both TOF and TON decreased substantially for complexes **6** and **7** (entries 5, 6). Interestingly, complex **8** featuring a tridentate coordinating bis-PYE ligand revealed a catalytic profile that is reminiscent to that of the bidentate analogue **4**, namely very high activity in the first minutes (TOF_{max} = 400 h^{-1}), followed by a marked loss of activity with incomplete conversion (TON = 22, entry 7). It is therefore conceivable that complexes **4** and **8** form the same catalytically active species, in agreement with the proton-dependent switch of the bi- vs. tridentate ligand coordination mode (see above). The relevance of the metal and the bis-PYE ligand are demonstrated by the absence of any FA dehydrogenation in the absence of a catalyst (entry 8), and the poor catalytic performance of $[Pd(PPh_3)_2Cl_2]$, which lacks the bis-PYE ligand (entry 9). Overall, this catalyst screening suggests that the counterion is highly relevant, and that stronger donating ancillary ligands L are beneficial for catalytic activity. However, there is also a trade-off between high initial activity (complexes **4** and **8**) vs. high conversion (complex **3b**). The latter has been exploited further by lowering the catalyst loading from 1 mol% to 0.1 mol%. Under these conditions, conversion with **3b** is almost complete within 4 h (TON = 850), and the initial rate raised to a TOF_{max} = 500 h^{-1} (entry 10). Further reduction of the catalyst loading to 0.01 mol% resulted in low conversion after 6 h (TON of = 550), indicating efficient quenching of catalytic activity under these dilute conditions. Such a deactivation is also indicated by the decreased conversion rate (TOF_{max} = 220 h^{-1}; entry 11), and may be caused by impurities in solvent or reagents.

Complex **3b** was used to investigate the effect of the solvent, the NEt_3 ratio, and Lewis acid additives on the FA dehydrogenation (Table S1). Replacement of dioxane as a solvent by H_2O or toluene did not reveal any benefits with low TONs for the former and considerably reduced TONs and TOFs in the latter. Likewise, modification of the onset FA/NEt_3 ratio from the original 11:10 molar ratio to either lower or higher NEt_3 fraction (2:1 or 1:1.5) decreased the catalytic performance. Notably, an increased NEt_3 ratio led to slightly higher initial TOFs (130 h^{-1}), which may hint to a delicate role of the acid-base ratio for catalytic activity. The addition of Lewis acids has been recognized as an efficient method to assist FA activation.[36] However, when catalytic reaction with **3b** was performed in the presence of 10 mol% $LiBF_4$, $NaBF_4$ or KBF_4, FA dehydrogenation was complete suppressed. This outcome is corroborated by the inactivity of complex **3c**, the BPh_4^- analogue of **3b** and underlines the relevance of the counterion in this palladium-catalyzed process. In agreement with this notion, the catalytic activity of **3c** is almost fully rescued when NBu_4Cl (10 mol%) is added to the reaction mixture. The use of chloride salts as additives with **3b**, *viz.* LiCl, NaCl, or KCl, led to a slight drop of catalytic performance, indicating that alkali metals have an inhibiting rather than any promoting effect. The performance of **3b** is promising and its catalytic stability is largely surpassing other known homogeneous Pd complexes for FA dehydrogenation (40 TON at 40 °C).[15] Nonetheless, the activity and stability of **3b** is far inferior to state-of-the-art iron, ruthenium or iridium complex, which reach TON and TOF values that are 2—3 orders of magnitude higher.[25,26,28]

Role of the ligand motif

Selective ligand modifications were introduced to better understand the effect of specific fragments of the bis-PYE ligand on

the catalytic palladium center. To this end, complex **9** was prepared as a complex with the same two PYE donor sites (Scheme 4a), though lacking the central NH group. This modification prevents any *cis-trans* isomerization as observed for complexes **4** and **8** and keeps the PYE sites in a static *cis* coordination, though obviously changes the orientation of the PYE heterocycles relative to the palladium coordination plane. The complex was readily available from the phenylene bis-PYE ligand precursor described by Wright,[37] and $[PdCl_2(PPh_3)_2]$ under basic conditions. Complex **9** is spectroscopically similar to **3b** and features the characteristic non-equivalent N–CH_3 groups ($\delta_H = 3.64$ and 3.80). Structural comparison is difficult since crystallization of **9** has been unsuccessful so far, even upon exchanging the non-coordinated anion to BPh_4^-. Strikingly, the catalytic activity of this complex is considerably lower than that of **3b** with only modest initial turnover frequency ($TOF_{max} = 79\ h^{-1}$) and rapid deactivation (28 TON; Table 2, entries 1–3). This lower activity may be a consequence of the lower reactivity imparted by the truncated ligand architecture, or due to a reduced stability of the complex, or a combination of both these effects.

To probe the relevance of the central *NH* functionality, complex **10** comprising a methylated central nitrogen was prepared from the known bis-nitrophenyl substituted methylamine **Me–$(NO_2)_2$** (Scheme 4b).[38] Reduction of the nitro groups yielded an air-sensitive bis-aniline, which was directly used for PYE-functionalization and palladation. Only after metalation, the compound was sufficiently air-stable and was conveniently purified by column chromatography. Of note, attempts to directly methylate the bis-PYE precursor **1** with MeI or MeOTf were unsuccessful and only afforded the starting material, while reactions with complex **3b** or **4** induced methylation of the palladium-bound PYE nitrogen and concomitant metal dissociation. Complex **10** featured spectroscopic properties very similar to **3b**, for example, inequivalent N–CH_3 resonances at $\delta_H = 3.43$ and 3.53 and a singlet in the ^{31}P NMR spectrum at $\delta_P = 25.0$. Anion exchange to BPh_4^- was required to grow X-ray quality single crystals of **10** (Figure 5a).[19] The molecular structures of **10** is similar to that of **3c**, with essentially identical bond distances and angles around the palladium center. For instance, the distance between palladium and the nitrogen located *trans* to the phosphine ligand is 2.072(1) Å in **10** (cf. 2.068(3) Å in **3c**). Likewise, the bite angle of the cis-bidentate *N,N*-ligand is identical (N2–Pd–N4 82.63(12)° in **10** and analogous angle 82.90(12)° in **3c**). The most distinct difference is probably the dihedral angle between the two central phenylene rings, which is 59.46° in complex **10** and only 52.62° in **3c**. This angle suggests a stronger helical twist in the presence of a central N–Me group vs. a N–H unit (see above). In

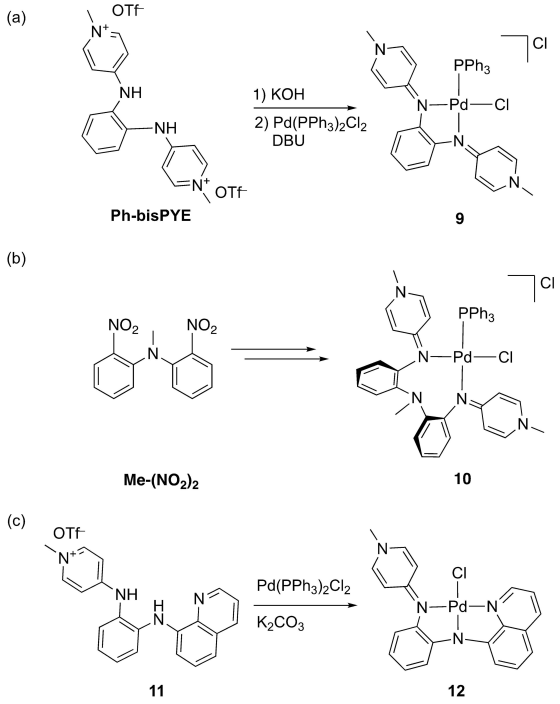

Scheme 4. Synthesis of complexes **9**, **10**, and **12** for comparison with bidentate ligated bis-PYE complex **3b** and the tridentate ligated bis-PYE complex **8**, respectively.

Table 2. Catalytic dehydrogenation of FA in presence of triethylamine.[a]

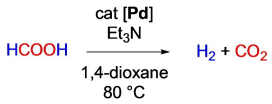

Entry	[Pd]	$V_{100\ min}$ [mL]	TON	TOF_{max} [h^{-1}][b]
1	**3b**	48.0	100	115
2	**8**	10.0	22	400
3	**9**	13.0	28	79
4	**10**	20.5	45	66
5	**12**	8.0	17	200

[a] Condition: catalyst (1 mol%), FA (1 mmol), Et_3N (0.91 mmol) and 1,4-dioxane (1 mL) at 80 °C for 100 min. [b] TOF maximum obtain from the catalytic profile.

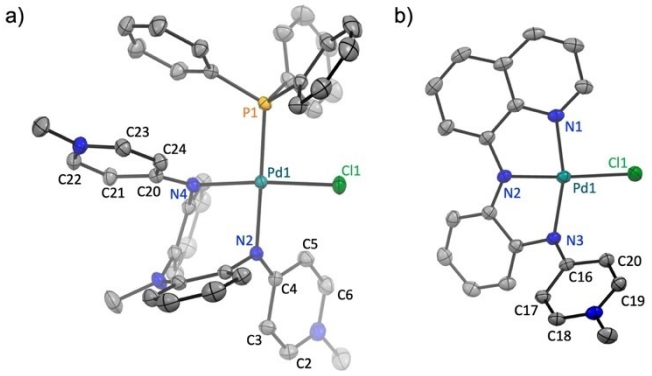

Figure 5. ORTEP representation of **10** (a) and **12** (b) at 50% probability level (all hydrogen atoms and BPh_4 anion of **10** omitted, rings below the coordination plane in lighter shade). Selected bond distances (Å) and bond angles (deg) for complex **10**: Pd1–Cl1 2.3076(3), Pd1–P1 2.2703(3), Pd1–N2 2.0724(10), Pd1–N4 2.0274(10), N4–C19 1.4227(14), N2–C7 1.4182(15), N4–C20 1.3221(15), N2–C4 1.3212(15), P1–Pd1–Cl1 88.830(11), N4–Pd1–N2 82.63(12), N4–Pd1–P1 95.3(3), N2–Pd1–Cl1 92.45(3), C20–N4–C19 121.20(10), C7–N2–C4 122.15(10). For complex **12**: Pd1–Cl1 2.3372(4), Pd1–N1 2.0225(12), Pd1–N2 1.9661(12), Pd1–N3 2.0400(11), N3–C15 1.4247(18), N3–C16 1.3466(16), Cl1–Pd1–N1 94.62(4), N1–Pd1–N2 82.07(5), N2–Pd1–N3 81.65(5), N3–Pd1–Cl1 101.93(3), C16–N3–C15 119.39(12).

catalysis, the insertion of the methyl group negatively impacted the activity. Complex **10** reached only about half of the activity of the NH analogue **3b** with $TOF_{max} = 66\ h^{-1}$ and a maximum turnover of 45 (entry 4; cf. TOFmax = 100 h^{-1} and TON = 115 for **3b**). These data demonstrate a significant, though not an essential role of the NH functionality.

In a further modulation, one PYE moiety was replaced with a quinoline group in **11** (Scheme 4c). Metalation under basic conditions (K_2CO_3) afforded the pincer palladium complex **12**, with a *N,N,N*-tridentate coordinated mono-PYE ligand. This product outcome contrasts that of the bis-PYE complex **3b**, which does not undergo deprotonation of the central *NH* unit with K_2CO_3 but instead required KO*t*Bu as a stronger base. Therefore, complex **12** may serve as an analogue of complex **8**. Single crystals suitable for X-ray diffraction analysis were obtained from slow diffusion of pentane into a CH_2Cl_2 solution of **12**.[19] The molecular structures feature a palladium center in a slightly distorted square planar geometry due to the acute N1–Pd1–N3 angle (163.40(5) between the pincer 'arms' (Figure 5b). The bonding metrics around the N_{PYE} center are similar to those observed in complexes **3c**, **4** and **10**, for example, Pd1–N3 is 2.0400(11) Å, and the exocyclic N3–C16 bond is 1.3466(16) Å, substantially shorter than a N–C single bond. The Pd–N bond to the quinoline site is slightly shorter (Pd–N1 2.0255(12) Å) than to the PYE unit. In catalytic formic acid dehydrogenation, complex **12** showed a reaction profile reminiscent to complex **8**, though less potent, i.e., a high initial turnover frequency $TOF_{max} = 200\ h^{-1}$ (entry 5; cf. 400 h^{-1} with **8**), and rapid deactivation, giving low overall turnover numbers (TON = 17 vs. 22 for **8**).

These data suggest that the tridentate activation afford a burst of activity in the first seconds of the reaction that may results from the fast acid-base reaction of **8** with formic acid (Table 1, entry 7; cf. 400 h^{-1}). However, the bidentate complex is better suited for long-term activity, which may be due to the presence of the non-coordinating chloride ligand and the strongly donating ancillary ligand (Table 1, entry 4; cf. 400 h^{-1} and TON of 61 for **4**). Notably, the results indicate the absence of a bidentate–tridentate switch of the coordination mode in the catalytic cycle because of the low acidity of the *NH* moiety and the different catalytic profiles of **4** and **8**. The ancillary ligand influenced the activity and stability of the complex (PPh_3, > $P(OPh)_3$ > DMAP; Table 1, entry 2; cf. 115 h^{-1} and TON of 100 for **3b**), which may point to a better stability and steric shielding with strong σ-donors such as PPh_3. Moreover, these data demonstrate the importance of the *NH* moiety for the catalytic mechanism, which may tentatively be attributed to the promotion of hydrogen bonding between the FA substrate and the basic nitrogen site in solution.[39,40] Such N···H–O interactions are suppressed with complex **9**. With complex **3c**, protonation of the central nitrogen is supposed to afford a $-NH_2^+$ unit with two reactive protons for interaction with a putative palladium-bound hydride to liberate H_2. With the NMe analogue **10**, only one proton can react, which may rationalize the reduced activity of **10** compared to **3c** (Table 2, entry 1 and 4). The relevance of hydrogen bonding is also supported by the strong dependence of the non-coordinating anion on the catalytic activity (cf. activity of complexes **3a–c**, and rescued activity of complex **3c** upon chloride addition).

A catalytic mechanism involving protonation of the central nitrogen of complex **3** is reinforced by substoichiometric experiments. Thus, reaction of complex **3b** with 10 mol equiv FA revealed the formation of a new palladium complex by ^{1}H NMR spectroscopy, which has higher symmetry based on the equivalent N–CH_3 resonances (Figure S39), which points to either a fast ligand exchange process or a *cis*/*trans* isomerization. Moreover, the central nitrogen is unambiguously protonated based on the new singlet integrating for two protons at 9.80 ppm (*cf* $\delta_H = 8.86$ in complex **3b**). Also HR-MS revealed a $[M–HCOO]^+$ signal. This protonation is fully reversible and addition of a base such as Na_2CO_3 allows complex **3b** to be fully recovered (Figure S39 and 40).

Conclusion

We have disclosed a new nitrogen-based ligand containing two pyridylidene imide (PYE) coordination sites and its coordination to palladium. Due to the presence of a central NH group, the ligand can flexibly coordinate in a *cis*-bidentate mode, or in a meridional *N,N,N*-tridentate coordination mode. This change in coordination mode is acid–base-triggered, fully reversible, and it also swaps the PYE sites from mutual *cis* to *trans* positions, reminiscent to the coordination flexibility of the Xantphos ligand family. In addition to this steric flexibility, the electronic flexibility of the PYE donor sites has been exploited in the *cis* coordinated palladium complexes to establish a *trans* influence scale for ligands coordinated *trans* to the PYE ligand site. Specifically, the N–CH_3 group of the PYE unit offers a diagnostic probe to assess the *trans* ligand influence, as stronger donors lead to a higher contribution of the quinoidal PYE resonance form, which induces an upfield shift of the N–CH_3 resonances.

The bis-PYE palladium complexes catalyze the dehydrogenation of formic acid. While the activities are 2–3 orders of magnitude lower than the most active complexes known for this reaction, the enabling effect of the bis-PYE units are demonstrated by a series of control experiments, which also support a synergistic effect of the metal center with the non-coordinated NH unit for formic acid activation. Moreover, the tridentate bonding mode substantially enhances the initial conversion rates (400 h^{-1}), whereas the bidentate coordination mode imparts higher robustness, accomplishing higher turnover numbers up to 850. These ligand design principles may provide guidelines for further catalytic applications, also using other metals in combination with this coordinatively and electronically flexible ligand system.

Experimental Section

Supporting Information Available: Detailed synthetic procedures and analytical data (^{1}H, ^{13}C, ^{19}F, ^{31}P NMR, elemental analysis and HRMS) of **1–12**.

All Crystals Structures have been deposited on the Cambridge Crystallographic Structural Database with Deposition Numbers 2167861 (for **3c**), 2167861 (for **4**), 2190523 (for **10**), and 2190523 (for **12**) containing the supplementary crystallographic data for this paper. These data are provided free of charge by the joint Cambridge Crystallographic Data Centre and Fachinformationszentrum Karlsruhe Access Structures service.

Acknowledgements

We acknowledge generous financial support from the Swiss National Science Foundation (grant 200020 182663). We thank the group of Chemical Crystallography of the University of Bern for X-ray analysis of all reported structures and Y. Kong and P. Broekmann (Univ Bern) for GC analyses. Open Access funding provided by Universität Bern.

Conflict of Interest

The authors declare no conflict of interest.

Data Availability Statement

The data that support the findings of this study are available in the supplementary material of this article.

Keywords: cis/trans coordination · formic acid dehydrogenation · hemilability · palladium · pyridylideneamines

[1] A. J. L. Pombeiro, *Dalton Trans.* **2019**, *48*, 13904–13906.
[2] Q. Shi, R. J. Thatcher, J. Slattery, P. S. Sauari, A. C. Whitwood, P. C. McGowan, R. E. Douthwaite, *Chem. Eur. J.* **2009**, *15*, 11346–11360.
[3] J. Slattery, R. J. Thatcher, Q. Shi, R. E. Douthwaite, *Pure Appl. Chem.* **2010**, *82*, 1663–1671.
[4] M. Navarro, C. A. Smith, M. Albrecht, *Inorg. Chem.* **2017**, *56*, 11688–11701.
[5] M. Navarro, M. Li, S. Bernhard, M. Albrecht, *Dalton Trans.* **2018**, *47*, 659–662.
[6] V. Leigh, D. J. Carleton, J. Olguin, H. Mueller-Bunz, L. J. Wright, M. Albrecht, *Inorg. Chem.* **2014**, *53*, 8054–8060.
[7] M. Navarro, M. Li, H. Müller-Bunz, S. Bernhard, M. Albrecht, *Chem. Eur. J.* **2016**, *22*, 6740–6745.
[8] M. E. Doster, S. A. Johnson, *Angew. Chem. Int. Ed.* **2009**, *48*, 2185–2187; *Angew. Chem.* **2009**, *121*, 2219–2221.
[9] P. D. W. Boyd, L. J. Wright, M. N. Zafar, *Inorg. Chem.* **2011**, *50*, 10522–10524.
[10] P. Melle, J. Thiede, D. A. Hey, M. Albrecht, *Chem. Eur. J.* **2020**, *26*, 13226–13234.
[11] D. G. A. Verhoeven, M. Albrecht, *Dalton Trans.* **2020**, *49*, 17674–17682.
[12] K. Salzmann, C. Segarra, M. Albrecht, *Angew. Chem. Int. Ed.* **2020**, *59*, 8932–8936; *Angew. Chem.* **2020**, *132*, 9017–9021.
[13] S. Bertini, D. Henryon, A. J. F. Edmunds, M. Albrecht, *Org. Lett.* **2022**, *24*, 1378–1382.
[14] P. Braunstein, F. Naud, *Angew. Chem. Int. Ed.* **2001**, *40*, 680–699; *Angew. Chem.* **2001**, *113*, 702–722.
[15] J. Broggi, V. Jurčík, O. Songis, A. Poater, L. Cavallo, A. M. Z. Slawin, C. S. J. Cazin, *J. Am. Chem. Soc.* **2013**, *135*, 4588–4591.
[16] S. Enthaler, A. Brück, A. Kammer, H. Junge, E. Irran, S. Gülak, *ChemCatChem* **2015**, *7*, 65–69.
[17] H. Wiener, Y. Sasson, J. Blum, *J. Mol. Catal.* **1986**, *35*, 277–284.
[18] T. Wu, S. N. MacMillan, K. Rajabimoghadam, M. A. Siegler, K. M. Lancaster, I. Garcia-Bosch, *J. Am. Chem. Soc.* **2020**, *142*, 12265–12276.
[19] CCDC 2167861, 2167861, 2190523 and 2190524 contain the supplementary crystallographic data for this paper. These data can be obtained free of charge from The Cambridge Crystallographic Data Centre. Deposition Numbers 2167861, 2167861, 2190523 and 2190524 contain the supplementary crystallographic data for this paper. These data are provided free of charge by the joint Cambridge Crystallographic Data Centre and Fachinformationszentrum Karlsruhe Access Structures service.
[20] a) G. van Koten, D. Milstein, *Top. Organomet. Chem.* **2013**, *40*, 1–2; b) M. Albrecht, G. van Koten, *Angew. Chem. Int. Ed.* **2001**, *40*, 3750–3781; *Angew. Chem.* **2001**, *113*, 3866–3898.
[21] a) P. W. N. M. van Leeuwen, P. C. J. Kamer, J. N. H. Reek, P. Dierkes, *Chem. Rev.* **2000**, *100*, 2741–2770; b) P. C. J. Kamer, P. W. N. M. van Leeuwen, J. N. H. Reek, *Acc. Chem. Res.* **2001**, *34*, 895–904.
[22] M.-N. Birkholz, Z. Freixa, P. W. N. M. van Leeuwen, *Chem. Soc. Rev.* **2009**, *38*, 1099.
[23] D. Mellmann, P. Sponholz, H. Junge, M. Beller, *Chem. Soc. Rev.* **2016**, *45*, 3954–3988.
[24] A. Boddien, D. Mellmann, F. Gärtner, R. Jackstell, H. Junge, P. J. Dyson, G. Laurenczy, R. Ludwig, M. Beller, *Science* **2011**, *333*, 1733–1736.
[25] E. A. Bielinski, P. O. Lagaditis, Y. Zhang, B. Q. Mercado, C. Würtele, W. H. Bernskoetter, N. Hazari, S. Schneider, *J. Am. Chem. Soc.* **2014**, *136*, 10234–10237.
[26] Z. Wang, S.-M. Lu, J. Li, J. Wang, C. Li, *Chem. Eur. J.* **2015**, *21*, 12592–12595.
[27] J. J. A. Celaje, Z. Lu, E. A. Kedzie, N. J. Terrile, J. N. Lo, T. J. Williams, *Nat. Commun.* **2016**, *7*, 11308.
[28] S. Kar, M. Rauch, G. Leitus, Y. Ben-David, D. Milstein, *Nat. Catal.* **2021**, *4*, 193–201.
[29] A. Agapova, E. Alberico, A. Kammer, H. Junge, M. Beller, *ChemCatChem* **2019**, *11*, 1910–1914.
[30] C. Guan, Y. Pan, T. Zhang, M. J. Ajitha, K. Huang, *Chem. Asian J.* **2020**, *15*, 937–946.
[31] N. Onishi, R. Kanega, H. Kawanami, Y. Himeda, *Molecules* **2022**, *27*, 455.
[32] N. H. Anderson, J. Boncella, A. M. Tondreau, *Chem. Eur. J.* **2019**, *25*, 10557–10560.
[33] A. Léval, H. Junge, M. Beller, *Catal. Sci. Technol.* **2020**, *10*, 3931–3937.
[34] W. Zhou, Z. Wei, A. Spannenberg, H. Jiao, K. Junge, H. Junge, M. Beller, *Chem. Eur. J.* **2019**, *25*, 8459–8464.
[35] N. Lentz, A. Aloisi, P. Thuéry, E. Nicolas, T. Cantat, *Organometallics* **2021**, *40*, 565–569.
[36] J. E. Heimann, W. H. Bernskoetter, N. Hazari, *J. Am. Chem. Soc.* **2019**, *141*, 10520–10529.
[37] M. N. Zafar, S. Masood, G.-S. Chaudhry, T. S. T. Muhammad, A. F. Dalebrook, M. F. Nazar, F. P. Malik, E. U. Mughal, L. J. Wright, *Dalton Trans.* **2019**, *48*, 15408–15418.
[38] N. Hara, T. Saito, K. Semba, N. Kuriakose, H. Zheng, S. Sakaki, Y. Nakao, *J. Am. Chem. Soc.* **2018**, *140*, 7070–7073.
[39] S. Oldenhof, M. Lutz, B. de Bruin, J. Ivar van der Vlugt, J. N. H. Reek, *Chem. Sci.* **2015**, *6*, 1027–1034.
[40] S. Y. de Boer, T. J. Korstanje, S. R. La Rooij, R. Kox, J. N. H. Reek, J. I. van der Vlugt, *Organometallics* **2017**, *36*, 1541–1549.

Manuscript received: August 26, 2022
Accepted manuscript online: September 6, 2022
Version of record online: October 11, 2022